Implementation of an Improved Performance Integral $\mathcal{H}_2/\mathcal{H}_\infty$ Combined Predictive Control on a GSP

Mahdy Rezaei Darestani[*1], AmirAli Nikkhah[2], Ali KhakiSedigh[3]

Received: 2014/7/5 Accepted: 2015/3/1

Abstract

to enhance the closed loop performance in presence of disturbance, uncertainties and delay a double loop mixture of MPC and robust controller is proposed. This double loop controller ensures smooth tracking for a 3-axis gyro-stabilized platform which has delay intrinsically. This control idea is suggested to eliminate high frequency disturbances and minimize steady state error with minimum power consumption in simulation and experiment. Proposed controller based on the combination of $\mathcal{H}_2$ and $\mathcal{H}_\infty$ controllers in the inner control loop shows the robustness of the proposed methodology. In the outer loop to have a good tracking performance, an integrated MPC is used to handle delay in system dynamics. Also, the main idea for dealing with uncertainties is using integral and derivative of platform attitude. In the proposed platform, the $\mathcal{H}_\infty$ controller is compared with $\mathcal{H}_\infty/\mathcal{H}_2$ controller in KNTU laboratory in theory and experiment. Results of experimental set up shows the same reaction of two controllers against disturbance and uncertainties in delayed system.

Keywords 3-axis GSP, predictive control, $\mathcal{H}_2/\mathcal{H}_\infty$ control, double loop controller

Introduction

As using the experimental test results are a proper technique to proof the reliability of a theoretical method, the proposed control algorithm which derived recently [24], implemented on a 3-axis GSP[4].

As the combination of predictive and robust control has a prescribed approach to control of uncertain systems with various affecting disturbances and delays, this idea is presented. In recent years, the $\mathcal{H}_2$ and $\mathcal{H}_\infty$ controller design techniques have been widely studied. Both have strong theoretical basis and are efficient algorithms for synthesizing optimal and robust controllers. Their combination, the mixed $\mathcal{H}_2/\mathcal{H}_\infty$ allows combining intuitive quadratic performance specifications of the $\mathcal{H}_2$ synthesis with robust stability requirements specifications expressed by the $\mathcal{H}_\infty$ synthesis. Mixture of these controllers leads to a superior closed loop performance in presence of large uncertainties and disturbances [1, 4, 5, 6, 7, 9, and 10].

In this paper a double loop controller is proposed. In the inner loop a mixed $\mathcal{H}_2/\mathcal{H}_\infty$ controller synthesis technique based on linear matrix inequalities (LMIs) is used. This set up considered a dynamic output feedback controller with transformed input.

In the outer loop, tracking loop, a predictive controller proposed. This combination increases the performance and stability, compensates system disturbances in presence of unmodeled system uncertainties.

This idea proposed to solve drawbacks caused by real time servo motors and data acquisition delays, sensor output disturbances and uncertainties. Also, some unmodeled dynamics because of channels coupling existed in the system.

Having a good performance in tracking as the control effort is minimized, has a very importance for the GSP. Reach to this criterion gets servo motors required power as low as possible. This criterion has a direct effect on the size of servo motors.

There is a rich literature in this area of control system design. These studies include, robust output feedback controller for the mixed $\mathcal{H}_2/\mathcal{H}_\infty$ controller. Based on Genetic Algorithms (GAs) and linear matrix inequalities (LMIs), a hybrid algorithm for uncertain continuous-time linear systems is presented [1]. To overcome the need for multivariable method of designing controller of low order, direct reduced order mixed $\mathcal{H}_2/\mathcal{H}_\infty$ control for the short take-off and landing maneuver technology is demonstrated [2]. Mixed $\mathcal{H}_2/\mathcal{H}_\infty$ control problem with reduced order controllers for time-varying systems in terms of the solvability of differential linear matrix inequalities and rank conditions is provided [3]. A mixed $\mathcal{H}_2/\mathcal{H}_\infty$ controller synthesis technique based on multi-objective optimization is used, where the optimized criteria are the $\mathcal{H}_2$ and $\mathcal{H}_\infty$ norms [4]. For a class of singular problems, necessary and sufficient conditions are established, so that the posed simultaneous $\mathcal{H}_2/\mathcal{H}_\infty$ problem is solvable by using state feedback controllers [5]. Fixed-structure discrete-time $\mathcal{H}_2/\mathcal{H}_\infty$ controller synthesis problem in the delta operator frame work is considered [6]. A new approach to mixed $\mathcal{H}_2/\mathcal{H}_\infty$ output

1.Aerospace Department, Khaje Nasir Toosi University of Technology, Tehran, Iran. m.rezaei.d@gmail.com
2.Aerospace Department, Khaje Nasir Toosi University of Technology, Tehran, Iran.nikkhah@kntu.ac.ir
3. Electrical and Computer Department, Khaje Nasir Toosi University of Technology, Tehran, Iran.sedigh@kntu.ac.ir

4 . gyro stabilized platform

feedback control synthesis is proposed. Using non-smooth mathematical programming techniques to compute locally optimal $\mathcal{H}_2/\mathcal{H}_\infty$ controllers, which may have a pre-defined structure, is presented [7]. A robust hybrid motion/force controller for rigid robot manipulators is presented. The main contribution of this study is to accomplish motion objectives in free directions and force objectives in constrained directions under parametric uncertainty [8]. LTI[1] and qLPV[2] $\mathcal{H}_2/\mathcal{H}_\infty$ controllers compared. The Pareto limit is used to show the compromise that has to be done when a mixed synthesis is achieved [9]. A stochastic $\mathcal{H}_\infty$ and a mixed, stochastic, $\mathcal{H}_2/\mathcal{H}_\infty$ control problem for discrete-time systems are considered and solved. Conditions for existence of a solution are derived, based on the solvability of an equivalent mini-max problem [10]. A collection of methods for improving the speed of MPC, using online optimization is described. These custom methods, which exploit the particular structure of the MPC problem, can compute the control action on the order of 100 times faster than a method that uses a generic optimizer [11], and so on [12, 13, and 14].

Here an IPI[3] combination of robust optimal control to have a smooth tracking, a model predictive controller (MPC) and a mixed $\mathcal{H}_2/\mathcal{H}_\infty$ control to high frequency disturbance rejection proposed. A transformed cost function input vector for a 3-axis GSP is proposed.

This paper is organized as follows. In section two, 3-axis GSP model derived. In section three, four and five, robust and optimal control theory and their combination is extended. In section six, the simulation results of the robust optimal methodologies to control and stabilize of the system are demonstrated. Finally this control strategy implemented on a real time 3-axis GSP.

Three-axis GSP modeling

With the use of mechanical gyros in a GSP structure, its model has been derived. The mathematical model of the mechanical gyro is based on the Euler equation of motion for a solid object where its center of mass is located on its center of rotation. Symbolic equation of motion is [15]:

$$M = \dot{H} + \omega \times H \quad (1)$$

This type of gyro stabilized platform consists of 3 single axis stabilizers. In this arrangement sensitive axis of each gyro is in direction of each axis of the stabilized platform. In relation to the sensed deviation of input axis of gyro, moment has been exerted to the related axis of platform to stabilize that axis. The main problem of a 3-axis GSP is input and output axis coupling of each channel.

In this stabilizer which its schematic view and gyros structure is shown in 0and 0, q angle is related to the precision axis and f is related to the rotation of input axis of stabilized platform gyros. As the structure of gyros on the platform is as in 0, the output angle of 3 axes is derived as the equation (8)-(10). By considering axis coupling and use of single axis stabilized gyro, state space equation of motion of 3-axis gyro stabilized platform has been derived for each channel [15].

X channel:

$$s^2.f_x = \frac{T_{nx}}{J_y} \quad (2)$$

$$(I.s^2 + D.s + K)q_z = H_y.s.f_x + U_p \quad (3)$$

Y channel:

$$s^2.f_y = \frac{T_{ny}}{J_y} \quad (4)$$

$$(I.s^2 + D.s + K)q_x = H_z.s.f_y + U_p \quad (5)$$

$$s^2.f_z = \frac{T_{nz}}{J_y} \quad (6)$$

$$(I.s^2 + D.s + K)q_y = H.s.f_z + U_p \quad (7)$$

Z channel:

And considering the channels coupling of the stabilized platform, the channels outputs are:

$$s_x = q_z + f_z \quad (8)$$

$$s_y = q_x + f_x \quad (9)$$

$$s_z = q_y + f_y \quad (10)$$

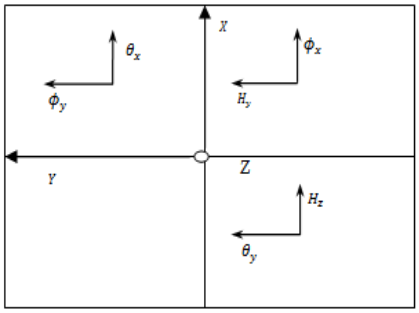

Figure 1. Gyro axis orientation on platform

Also, the control signals and the disturbances of each channel are respectively [15]:

$$T_{ni} = T_{di} - T_{si} \quad (11)$$

As previously stated, the input moment causes to precision of gyro to sense the q angle. This sensor is installed in each channel of the stabilizer, as stated in figure (2), and the state space equation of a 3-axis platform is derived as follows:

$$\dot{\bar{X}} = A\bar{X} + B\bar{U} + \bar{U}_f \quad (12)$$

1. Linear Time Invariant

2. Quadratic Linear Parameter Varying

3. improved performance integrated

$$\bar{Y} = C\bar{X} \tag{13}$$

$$\bar{X} = \begin{bmatrix} \phi_x \\ \dot{\phi}_x \\ \theta_z \\ \dot{\theta}_z \\ \phi_y \\ \dot{\phi}_y \\ \theta_x \\ \dot{\theta}_x \\ \phi_z \\ \dot{\phi}_z \\ \theta_y \\ \dot{\theta}_y \end{bmatrix}; \quad \bar{U} = \begin{bmatrix} T_{nx} \\ T_{ny} \\ T_{nz} \end{bmatrix}; \quad \bar{Y} = \begin{bmatrix} \sigma_x \\ \sigma_y \\ \sigma_z \end{bmatrix} = \begin{bmatrix} \theta_z + \phi_z \\ \theta_x + \phi_x \\ \theta_y + \phi_y \end{bmatrix} \tag{14}$$

$$A = \begin{bmatrix} \begin{bmatrix} 0 & 1 & 0 & 0 \\ -\frac{K_x}{I_x} & -\frac{D_x}{I_x} & 0 & 0 \\ 0 & 0 & 0 & 1 \\ 0 & \frac{H}{I} & -\frac{K}{I} & -\frac{D}{I} \end{bmatrix} & 0 & 0 \\ 0 & \begin{bmatrix} 0 & 1 & 0 & 0 \\ -\frac{K_y}{I_y} & -\frac{D_y}{I_y} & 0 & 0 \\ 0 & 0 & 0 & 1 \\ 0 & \frac{H}{I} & -\frac{K}{I} & -\frac{D}{I} \end{bmatrix} & 0 \\ 0 & 0 & \begin{bmatrix} 0 & 1 & 0 & 0 \\ -\frac{K_z}{I_z} & -\frac{D_z}{I_z} & 0 & 0 \\ 0 & 0 & 0 & 1 \\ 0 & \frac{H}{I} & -\frac{K}{I} & -\frac{D}{I} \end{bmatrix} \end{bmatrix} \tag{15}$$

$$B = \begin{bmatrix} 0(1,3) & & \\ \frac{1}{J_x} & 0 & 0 \\ 0(3,3) & & \\ 0 & \frac{1}{J_y} & 0 \\ 0(3,3) & & \\ 0 & 0 & \frac{1}{J_z} \\ 0(2,3) & & \end{bmatrix}, U_f = \begin{bmatrix} 0 \\ 0 \\ 0 \\ \frac{U_{px}}{I_x} \\ 0 \\ 0 \\ 0 \\ \frac{U_{py}}{I_y} \\ 0 \\ 0 \\ 0 \\ \frac{U_{pz}}{I_z} \end{bmatrix}, \tag{16}$$

$$C = \begin{bmatrix} 0 & 0 & 1 & 0(1,5) & & & & & 1 & 0 & 0 & 0 \\ 1 & 0(2,3) & & & 0 & 0 & 1 & 0(2,3) & & & 0 & 0 \\ 0 & & & & 1 & 0 & 0 & & & & 1 & 0 \end{bmatrix}$$

A controller to stabilize and ensure closed loop tracking of the linear time invariant model of the gyro-stabilized system must now be designed.

$$U = U_0 - U_c \qquad (17)$$

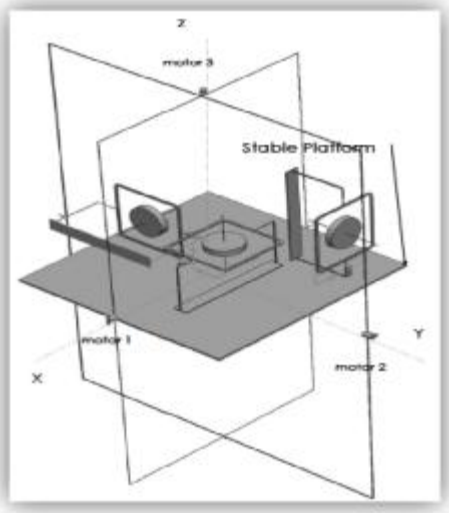

Figure 2. Schematic of 3-axis stabilized platform

GSP Control Idea

The proposed controller for the 3-axis GSP is a mixed controller. This combination is a double loop controller (DLC) that uses $\mathcal{H}_2/\mathcal{H}_\infty$ in the inner loop. A predictive control in the outer loop is proposed. Integral/derivative of platform attitude accounted in cost function.

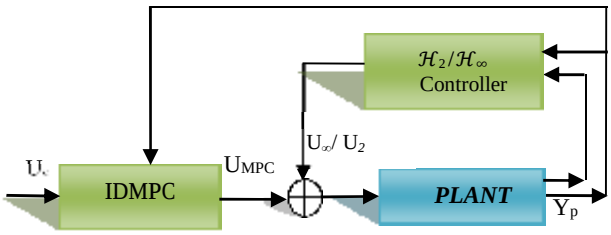

Figure 3. Proposed controller block diagram for the stabilized platform

This combination uses benefits of predictive control to have a smooth tracking and reduction of low frequency time variant disturbances of a pre-defined trajectory. A mixed $\mathcal{H}_2/\mathcal{H}_\infty$ controller to handle unknown uncertainties and compensating high frequency disturbances considered. This combination minimizes control force with the use of proposed DLC. The $\mathcal{H}_2/\mathcal{H}_\infty$ controller gains derived in MATLAB with LMI theory. [16, 18, 19]

Also, in predictive control with considering instantaneous receding horizon, system could overcome the sudden increase of input control signal and instability. 0shows block diagram of the proposed controller for the 3-axis GSP.

ID[1] Predictive Control

Predictive control is an optimal controller and provides high accuracy in tracking of the desired trajectory. The stabilized platform attitude could reach to the desired attitude with a high accuracy by considering some criteria. In this case, proper selection of sensors and well selected structure of optimal controller is very important. In the second step with implementation of input commands, in the case of output disturbances, could reach to the desired accuracy of the system. In what follows, the cost function of the model predictive control (MPC), and the Integral/derivative characteristics of the error are given. To design the predictive control state space equation of the 3-axis GSP is used [13, 14]:

$$\dot{\boldsymbol{X}} = F(\boldsymbol{X}, \boldsymbol{U}) = \mathbf{A}.\mathbf{X}(\mathbf{t}) + \mathbf{B}.\boldsymbol{U}(\boldsymbol{t}) \qquad (18)$$

$$\boldsymbol{Y} = \begin{bmatrix} \sigma_x \\ \sigma_y \\ \sigma_z \end{bmatrix} = G(\boldsymbol{X}) = \boldsymbol{C}.\boldsymbol{X} \qquad (19)$$

To control the stabilized platform it is assumed that the proposed platform is fixed on a set point or moves with an external command U_{Pi} (usually $U_{Pi} \approx 0$ in controller design) to a defined position. So a predefined trajectory for equation of motion of body without disturbances in ideal condition as the reference model is considered [14, 15, 16]:

$$\dot{\boldsymbol{X}}_{\boldsymbol{r}}(\mathrm{t}) = \mathrm{F}(\boldsymbol{X}_{\boldsymbol{r}}, \boldsymbol{U}_{\boldsymbol{r}}) = \mathbf{A}.\boldsymbol{X}_{\boldsymbol{r}}(\mathrm{t}) + \mathbf{B}.\boldsymbol{U}_{\boldsymbol{r}}(\mathrm{t}) \qquad (20)$$

$$\boldsymbol{Y}_{\boldsymbol{r}} = \mathrm{G}(\boldsymbol{X}_{\boldsymbol{r}}) = \mathbf{C}.\boldsymbol{X}_{\boldsymbol{r}} \qquad (21)$$

1. Integral Derivative

Where U_{ri} is the input reference moment and Y_{ri} is the output reference angle in each axis of the stable platform. This reference model has been used to define control input variations of the system in all conditions with or without disturbance. With these two defined models the error equation of the system is derived [12]:

$$\dot{\boldsymbol{X}}_{\boldsymbol{\zeta}}(t) = F\left(\boldsymbol{X}_{\boldsymbol{\zeta}}, \boldsymbol{U}_{\boldsymbol{\zeta}}\right) = \mathbf{A}.\boldsymbol{X}_{\boldsymbol{\zeta}}(t) + \mathbf{B}.\boldsymbol{U}_{\boldsymbol{\zeta}}(t) \quad (22)$$

$$\boldsymbol{Y}_{\boldsymbol{\zeta}} = G\left(\boldsymbol{X}_{\boldsymbol{\zeta}}\right) = \mathbf{C}.\boldsymbol{X}_{\boldsymbol{\zeta}} \quad (23)$$

Now to reach to the desired control specifications, output error vector which consists of integral and derivative of the output error is:

$$\widetilde{\boldsymbol{Y}}_{\boldsymbol{\zeta}} = H\left(\bar{\bar{\boldsymbol{X}}}_{\boldsymbol{n}}\right) = \begin{bmatrix} \tilde{\tau}_x \\ \dot{\tilde{\tau}}_x \\ \int \tilde{\tau}_x\, dt \\ \tilde{\tau}_y \\ \dot{\tilde{\tau}}_y \\ \int \tilde{\tau}_y\, dt \\ \tilde{\tau}_z \\ \dot{\tilde{\tau}}_z \\ \int \tilde{\tau}_z\, dt \end{bmatrix} = \begin{bmatrix} \sigma_x - \sigma_{xr} \\ \dot{\sigma}_x - \dot{\sigma}_{xr} \\ \int (\sigma_x - \sigma_{xr})dt \\ \sigma_y - \sigma_{yr} \\ \dot{\sigma}_y - \dot{\sigma}_{yr} \\ \int (\sigma_y - \sigma_{yr})dt \\ \sigma_z - \sigma_{zr} \\ \dot{\sigma}_z - \dot{\sigma}_{zr} \\ \int (\sigma_z - \sigma_{zr})dt \end{bmatrix} \quad (24)$$

$$C_{MPC} = \begin{bmatrix} \begin{bmatrix} 0 & t_{12} & 0 \\ t_{11} & t_{12} & t_{13} \\ 0 & 0 & t_{13} \end{bmatrix} & 0 & 0 \\ 0 & \begin{bmatrix} 0 & t_{22} & 0 \\ t_{21} & t_{22} & t_{23} \\ 0 & 0 & t_{23} \end{bmatrix} & 0 \\ 0 & 0 & \begin{bmatrix} 0 & t_{32} & 0 \\ t_{31} & t_{32} & 0 \\ 0 & 0 & t_{33} \end{bmatrix} \end{bmatrix} \quad (25)$$

$$, B_{MPC} = \begin{bmatrix} 0 \\ 1 \\ 0 \end{bmatrix}$$

In the steady state, as $(t \to \infty)$, the output controlled error tend to reach to zero $(YV \to 0)$ and decreases the error of the whole system, as the system output tracks the reference path. Here, $T_i = [t_{i1}, t_{i2}, t_{i3}]$ is considered as [22]:

$$t_{i1} = 1 + k_{1p}.\left(1 - sech\left(k_{2p}.e\right)\right) \quad (26)$$

$$\boldsymbol{t_{i2}} = \boldsymbol{k_D}.\Big[\boldsymbol{s(e.\dot{e})}.\left(\boldsymbol{k_{0D}} + \boldsymbol{k_{1D}}.(\mathbf{1} - \boldsymbol{sech}(\boldsymbol{k_{2D}}.\boldsymbol{e}))\right) + \frac{\boldsymbol{k_h}}{\mathbf{1} + \boldsymbol{\mu^2}.\boldsymbol{e^2}}\Big] \quad (27)$$

$$t_{i3} = \frac{1}{1 + exp[\beta.(-\alpha.e) - 0.1]} - \frac{1}{1 + exp[\beta.(-\alpha.e) + 0.1]} \quad (28)$$

The proposed controller is optimal with minimum energy consumption and could compensate output error changing. This condition with minimizing the following cost function in the proposed MPC has been assessed [13, 14].

$$J_z = \left[\tilde{Y}_{\zeta} - \tilde{Y}_{\zeta r}\right]' Q\left[\tilde{Y}_{\zeta} - \tilde{Y}_{\zeta r}\right] + \left[\tilde{u}_{\zeta} - \tilde{u}_{\zeta r}\right]'. .R\left[\tilde{u}_{\zeta} - \tilde{u}_{\zeta r}\right] + \Omega\left\{\tilde{Y}_{\zeta}(k+N|k) - \tilde{Y}_{\zeta r}(k+N|k)\right\} \quad (29)$$

Where R and Q are diagonal positive definite weighting matrices and N is the control horizon. Also Ω is the cost of final states in the predictive system which is explained as [12, 14]:

$$\Omega\left\{\widetilde{\boldsymbol{Y}}_{\boldsymbol{\zeta}}(k+N|k) - \widetilde{\boldsymbol{Y}}_{\boldsymbol{\zeta r}}(k+N|k)\right\} = \left[\widetilde{\boldsymbol{Y}}_{\boldsymbol{\zeta}}(k+N|k) - \widetilde{\boldsymbol{Y}}_{\boldsymbol{\zeta r}}(k+N|k)\right]' Q_{\zeta}. \left[\widetilde{\boldsymbol{Y}}_{\boldsymbol{\zeta}}(k+N|k) - \widetilde{\boldsymbol{Y}}_{\boldsymbol{\zeta r}}(k+N|k)\right] \quad (30)$$

And in the above equation Q_{ζ} is positive definite. Input/output prediction of the future step of discrete model of the system is [13]:

$$\widehat{\widetilde{\boldsymbol{u}}}_{\boldsymbol{\zeta}} = \begin{bmatrix} \tilde{u}_{\zeta_r}(k+1|k) - \tilde{u}_{\zeta_r}(k|k) \\ \vdots \\ \tilde{u}_{\zeta_r}(k+N+1|k) - \tilde{u}_{\zeta_r}(k|k) \end{bmatrix} \quad (31)$$

$$\widetilde{\boldsymbol{Y}}_{\boldsymbol{\zeta}} = \begin{bmatrix} \tilde{Y}_{\zeta_r}(k+1|k) - \tilde{Y}_{\zeta_r}(k|k) \\ \vdots \\ \tilde{Y}_{\zeta_r}(k+N+1|k) - \tilde{Y}_{\zeta_r}(k|k) \end{bmatrix} \quad (32)$$

And,

$$\begin{bmatrix} Y_{\zeta_{k+1}} \\ Y_{\zeta_{k+2}} \\ \vdots \\ Y_{\zeta_{k+N}} \end{bmatrix} = \begin{bmatrix} CA \\ CA^2 \\ \vdots \\ CA^N \end{bmatrix} \bar{\tilde{X}}_{\zeta} + \quad (33)$$

$$+ \begin{bmatrix} \boldsymbol{CB} & \boldsymbol{0} & \cdots & \boldsymbol{0} \\ \boldsymbol{CAB} & \boldsymbol{CB} & \cdots & \boldsymbol{0} \\ \vdots & \vdots & \cdots & \vdots \\ \boldsymbol{CA^{N-1}B} & \cdots & \boldsymbol{CA^{N-L}B} & \boldsymbol{0} \end{bmatrix} . \begin{bmatrix} \widehat{\widetilde{\boldsymbol{u}}}_{\boldsymbol{\zeta_k}} \\ \widehat{\widetilde{\boldsymbol{u}}}_{\boldsymbol{\zeta_{k+1}}} \\ \vdots \\ \widehat{\widetilde{\boldsymbol{u}}}_{\boldsymbol{\zeta_{k+L}}} \end{bmatrix}$$

$$\boldsymbol{Y_{\xi}(k+j)} = S_{\zeta}\boldsymbol{X_{\xi}(k+j)} + H.\boldsymbol{u_{\xi}(k+j)} \quad (34)$$

Minimizing the cost function of the predictive control without the constraints results to the following control law and this control signal has been used in the input control signal of the equation of motion of the system [12, 13, and 14]:

$$\widehat{\widetilde{\boldsymbol{u}}}_{\boldsymbol{\xi}} = [\boldsymbol{H'QH} + \boldsymbol{R}]^{-1}.\Big[\boldsymbol{H'Q}\Big(\widehat{\boldsymbol{Y}}_{\boldsymbol{\xi r}} - \boldsymbol{S_{\zeta}X_{\xi}(k)}\Big) + \boldsymbol{R}\widehat{\widetilde{\boldsymbol{u}}}_{\boldsymbol{\xi r}}\Big] \quad (35)$$

That in every sampling time, k, only $\widehat{\widetilde{\boldsymbol{u}}}_{\boldsymbol{\xi}}$ signal is required. Finally, the resulted control signal is used in the GSP, with uncertainty and delay, to reach an appropriate tracking.

Mixed $\mathcal{H}_2/\mathcal{H}_\infty$ Controller

In this section, an integration of a special type of robust optimal control, mixed $\mathcal{H}_2/\mathcal{H}_\infty$ control is presented. This control loop stabilizes the platform. This controller is considered in the inner loop of DLC. It could compensate all the unknown high frequency disturbances existed in the GSP or generated in the tracking loop of the predictive control. Advantage of the proposed controller is minimum control effort. This process must consider system optimal control signal boundary, especially in the presence of disturbances. So, it is [12, 20]:

$$\dot{X} = AX + B_{\infty}w_{\infty} + B_2w_2 + B_uU \quad (36)$$

$$Z_{\infty} = C_{\infty}X + D_{\infty\infty}w_{\infty} + D_{\infty 2}w_2 + D_{\infty u}U \quad (37)$$

$$Z_2 = C_2X + D_{2\infty}w_{\infty} + D_{22}w_2 + D_{2u}U \quad (38)$$

$$Y = C_yX + D_{y\infty}w_{\infty} + D_{y2}w_2 + D_{yu}U \quad (39)$$

Where U is the input control vector, w_2 is the external structured disturbance vector, w_∞ is the unstructured external disturbance vector, X and Y, Z_2, Z_∞ are the state and output of the system. Let $D_{yu} = 0$ and to compute a finite value of the $\mathcal{H}_2$ norm $D_{22} = 0$. Also, generally $D_{\infty 2} = D_{2\infty} = 0$, so [19, 20 and 21]:

$$\dot{X} = AX + B_{\infty}w_{\infty} + B_2w_2 + B_uU \quad (40)$$

$$Z_{\infty} = C_{\infty}X + D_{\infty\infty}w_{\infty} + D_{\infty u}U \quad (41)$$

$$Z_2 = C_2X + D_{2u}U \quad (42)$$

$$Y = C_yX + D_{y\infty}w_{\infty} + D_{y2}w_2 \quad (43)$$

Here, for high frequency disturbance attenuation, control of the first order derivative of platform attitude has been considered. Also, as in MPC, proportional, derivative and integral sequence is used. In the inner loop rate of change of platform attitude error, as the control parameter in the error vector, has been considered. The integral term accomplishes zero steady state error when steady disturbance and uncertainty error affects the system. For the case of output-feedback, a dynamic controller is assumed for each part of the $\mathcal{H}_2$ and $\mathcal{H}_\infty$ controller. For the $\mathcal{H}_2$ controller:

$$\dot{x}_2 = A_{k2}x_2 + B_{k2}T_1y_{c1} \quad (44)$$

$$U_2 = C_{k2}z_2 + D_{k2}T_1y_{c1} \quad (45)$$

And for the $\mathcal{H}_\infty$ controller;

$$\dot{x}_{\infty} = A_{k\infty}x_{\infty} + B_{k\infty}T_2y_{c2} \quad (46)$$

$$U_{\infty} = C_{k\infty}z_{\infty} + D_{k\infty}T_1y_{c2} \quad (47)$$

$$K_{Ci}: \begin{bmatrix} A_{ki} & B_{ki} \\ C_{ki} & D_{ki} \end{bmatrix} \quad (48)$$

In the first step to design this controller, to stabilize the system in the inner loop and compensation of high frequency disturbances, the output error considered for the above outputs are:

$$\tilde{y}_{\chi} = \begin{bmatrix} \dot{\tilde{\chi}}_x \\ \ddot{\tilde{\chi}}_x \\ \int \dot{\tilde{\chi}}_x \, dt \\ \dot{\tilde{\chi}}_y \\ \ddot{\tilde{\chi}}_y \\ \int \dot{\tilde{\chi}}_y \, dt \\ \dot{\tilde{\chi}}_z \\ \ddot{\tilde{\chi}}_z \\ \int \dot{\tilde{\chi}}_z \, dt \end{bmatrix} = \begin{bmatrix} \dot{\sigma}_x - \dot{\sigma}_{xr} \\ \ddot{\sigma}_x - \ddot{\sigma}_{xr} \\ \int \dot{\sigma}_x - \dot{\sigma}_{xr} \, dt \\ \dot{\sigma}_y - \dot{\sigma}_{yr} \\ \ddot{\sigma}_y - \ddot{\sigma}_{yr} \\ \int \dot{\sigma}_y - \dot{\sigma}_{yr} dt \\ \dot{\sigma}_z - \dot{\sigma}_{zr} \\ \ddot{\sigma}_z - \ddot{\sigma}_{zr} \\ \int \dot{\sigma}_z - \dot{\sigma}_{zr} dt \end{bmatrix} = C_1 . \tilde{x}_{\chi} \quad (49)$$

$$C_1 = \begin{bmatrix} 0 & I(3) & 0 & 0 & I(3) & 0 \\ I(3) & 0 & 0 & I(3) & 0 & 0 \\ 0 & 0 & I(3) & 0 & 0 & I(3) \end{bmatrix} \quad (50)$$

$$\tilde{x}_{\chi} = \begin{bmatrix} \dot{\phi}_x - \dot{\phi}_{xr} \\ \ddot{\phi}_x - \ddot{\phi}_{xr} \\ \int \dot{\phi}_x - \dot{\phi}_{xr} dt \\ \dot{\theta}_z - \dot{\theta}_{zr} \\ \ddot{\theta}_z - \ddot{\theta}_{zr} \\ \int \dot{\theta}_z - \dot{\theta}_{zr} dt \\ \dot{\phi}_y - \dot{\phi}_{yr} \\ \ddot{\phi}_y - \ddot{\phi}_{yr} \\ \int \dot{\phi}_y - \dot{\phi}_{yr} dt \\ \dot{\theta}_x - \dot{\theta}_{xr} \\ \ddot{\theta}_x - \ddot{\theta}_{xr} \\ \int \dot{\theta}_x - \dot{\theta}_{xr} dt \\ \dot{\phi}_z - \dot{\phi}_{zr} \\ \ddot{\phi}_z - \ddot{\phi}_{zr} \\ \int \dot{\phi}_z - \dot{\phi}_{zr} dt \\ \dot{\theta}_y - \dot{\theta}_{yr} \\ \ddot{\theta}_y - \ddot{\theta}_{yr} \\ \int \dot{\theta}_y - \dot{\theta}_{yr} dt \end{bmatrix} \quad (51)$$

Therefore, the closed loop system is described as [21, 22 and 23].

$$\begin{bmatrix} \dot{X}_{cl} \\ Z_{\infty} \\ Z_2 \end{bmatrix} = \begin{bmatrix} A_{cl} & | & B_{cl\infty} & B_{cl2} \\ - & - & - & - \\ C_{cl\infty} & | & D_{cl\infty} & D_{cl2} \\ C_{cl2} & | & E_{cl\infty} & 0 \end{bmatrix} . \begin{bmatrix} X_{cl} \\ w_{\infty} \\ w_2 \end{bmatrix} \quad (52)$$

Where:

$$A_{cl} = \begin{bmatrix} A + B_u D_{kj} C_y & B_u C_{kj} \\ B_{kj} C_y & A_{kj} \end{bmatrix} \quad (53)$$

$$B_{cl\infty} = \begin{bmatrix} B_{\infty} + B_u D_k D_{y\infty} \\ B_k D_{y\infty} \end{bmatrix} \quad (54)$$

$$B_{cl2} = \begin{bmatrix} B_2 + B_u D_k D_{y2} \\ B_k D_{y2} \end{bmatrix} \quad (55)$$

$$C_{clj} = \begin{bmatrix} C_j + D_{ju} D_{kj} C_y & D_{ju} C_{kj} \end{bmatrix} \quad (56)$$

$$D_{cl\infty} = \begin{bmatrix} D_{\infty\infty} + D_{\infty u} D_{kj} D_{y\infty} \end{bmatrix} \quad (57)$$

$$D_{cl\infty} = \begin{bmatrix} D_{\infty 2} + D_{\infty u} D_{kj} D_{y2} \end{bmatrix} \quad (58)$$

$$E_{cl\infty} = \begin{bmatrix} D_{2u} D_{kj} D_{y\infty} + D_{2\infty} \end{bmatrix} \quad (59)$$

$$E_{cl2} = [0] \quad (60)$$

Using bounded real lemma and concept of the quadratic stability, the $\mathcal{H}_{\infty}$ constraint is equivalent to existence of a unique solution $X_{\infty} > 0$ that satisfies the matrix inequality:

$$\begin{pmatrix} A_{cl}^T X_{\infty} + X_{\infty} A_{cl} & X_{\infty} B_{cl\infty} & C_{cl\infty}^T \\ B_{cl\infty}^T X_{\infty} & -g_{\infty}^2 I & D_{cl\infty}^T \\ C_{cl\infty} & D_{cl\infty} & -I \end{pmatrix} < 0 \quad (61)$$

And for the $\mathcal{H}_2$ performance measure, the $\mathcal{H}_2$ norm of T_{z2w} is derived as:

$$\|T_{z2w}\|_2^2 = Trace\left(C_{cl2} X_2 C_{cl2}^T\right) \quad (62)$$

Where $X_2 > 0$ is the solution of the Lyapunov equation:

$$A_{cl} X_2 + X_2 A_{cl}^T + B_{cl} B_{cl}^T = 0 \quad (63)$$

That for the proposed uncertain system plant, $\|T_{z2w}\|_2^2 \le Trace(C_{cl2} X_2^* C_{cl2}^T)$ for any $X_2^* > 0$ such that:

$$A_{cl} X_2^* + X_2^* A_{cl}^T + B_{cl} B_{cl}^T < 0 \quad (64)$$

It is important to notice that the inequalities (61), (64) are LMIs dependent to the fixed controller gains (K_{Ci}) and g_{∞}, g_2.

Summarizing above relations derives integrated $\mathcal{H}_2/\mathcal{H}_{\infty}$ robust control problem matrix inequality as equation (61) and (65)-(67):

$$\begin{bmatrix} A_{cl}^T X_2^* + X_2^* A_{cl} & X_2^* B_{cl2} \\ B_{cl2}^T X_2^* & -I \end{bmatrix} < 0 \quad (65)$$

$$\begin{bmatrix} X_2^* & C_{cl2}^T \\ C_{cl2} & Y_2 \end{bmatrix} > 0 \quad (66)$$

$$Trace(Y_2) < g_2 \quad (67)$$

"As stated in the recent studies [22], this problem is not convex in the variables (X_2, X_{∞}, K_C), but it is convex for

a fixed controller K_{ci}. This performance criterion gives an upper bound of the optimal $\mathcal{H}_2$ performance subject to the $\mathcal{H}_\infty$ norm constraint. Here must be mentioned that this approach assumes the hypothesis of common Lyapunov matrices, as $X_2 = X_\infty$". "Its advantage is conservatism reduction and better results generation. "Also, the dynamic or static output feedback control case for plants subject to uncertainties is solvable". [21]

This problem solved by MATLAB LMI control toolbox by specified constraints. The combination of the $\mathcal{H}_2$ and $\mathcal{H}_\infty$ synthesis is done by combining equation (58), (65), (66) and (67) to a single LMI. A solution can be found again by setting γ_∞ to a desired, achievable value and solving a $Trace(Y_2)$ minimization problem [19, 20 and 21].

"Problem definition in relation to the proposed controller setup in MATLAB and finding a suitable gain (K(s)) with LMI control toolbox is introduced as the following steps" [19]:

Step 1: Plant definition as a MATLAB LTI system:

A= A ; B=$\begin{bmatrix} B_\infty & B_2 & B_u \end{bmatrix}$; C=$\begin{bmatrix} C_\infty & C_2 & C_u \end{bmatrix}$;

D=$\begin{bmatrix} D_{\infty\infty} & 0 & D_{\infty u}; & 0 & 0 & D_{2u}; & D_{y\infty} & 0 & D_{y2} \end{bmatrix}$,

P = ltisys (A, B, C, D)

, that P is the system plant.

Step 2: Determine the integrated $\mathcal{H}_2/\mathcal{H}_\infty$ controller gain, K(s):

- r =[3 3 3]; that is a 1×3 vector listing the lengths of z_2, y and u
- region-lmireg: Allows specify and place the closed-loop poles in the region that lmi calculation is doing.
- obj=[γ ν α β]: vector specifying the $\mathcal{H}_2/\mathcal{H}_\infty$ objective.

[gopt,h2opt,K]=hinfmix(P,r,obj,region)

, that optimal output-feedback controller gain, K, is defined with MATLAB functions [20, 21].

Finally by executing an optimal loop to choose the best control gain, a pareto limit diagram for each channel of GSP is derived. Optimal gain is where the performance of $\mathcal{H}_\infty$ and $\mathcal{H}_2$ get minimized at the same time. This point for different γ value marked in the following figures.

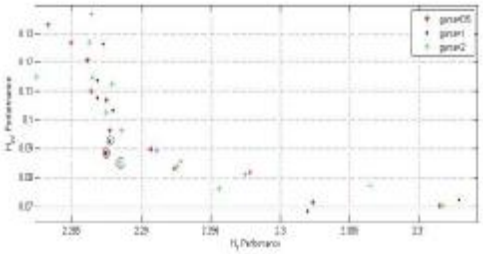

(a). roll channel

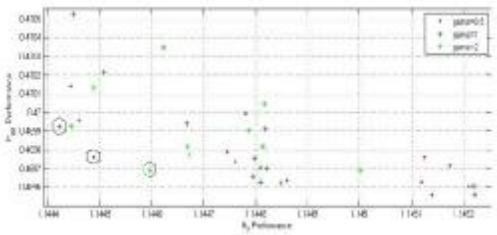

(b). pitch channel

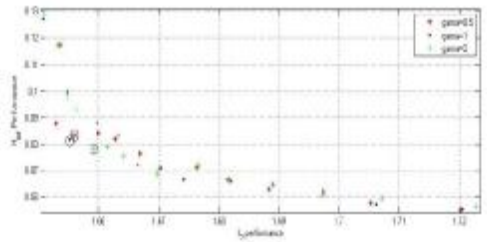

(c). yaw channel

Figure 4. Integrated controller pareto like diagram

GSP Simulation

System simulation is performed in two cases, with and without input stabilizing loop. A comparison study of the proposed controller and a NLPID control, [22], is performed. In the following simulation, results of the three-axis GSP simulation are presented.

In the first section simulation, results are without the inner stabilizing loop which shows good tracking without platform stabilizing that system oscillates at the equilibrium point due to the interaction dynamics. These results have been generated with the use of MPC and NLPID controller in the outer loop or tracking loop of GSP which tunes the attitude of the platform in relation to the predefined reference. As shown in 00and Figure 6, MPC generated control command and tracking path has the value and frequency lower than the NLPID control. Also the system oscillation in tracking mode is minimum.

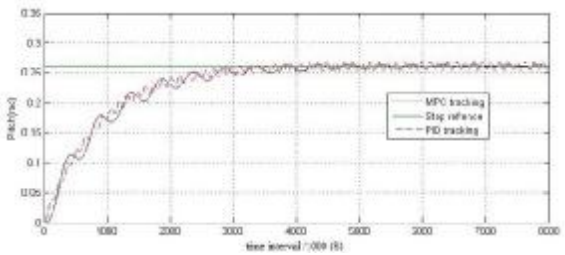

Figure 5. Comparison of NLPID Control and MPC Implementation Without Platform Stabilizing

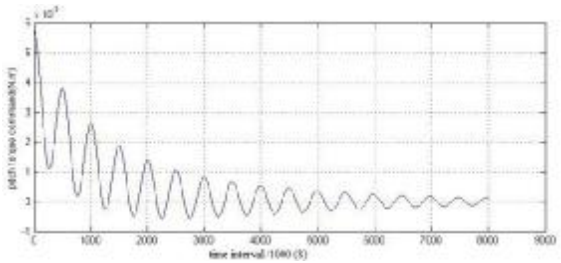

Figure 6. Pitch channel control command for MPC without platform stabilizing

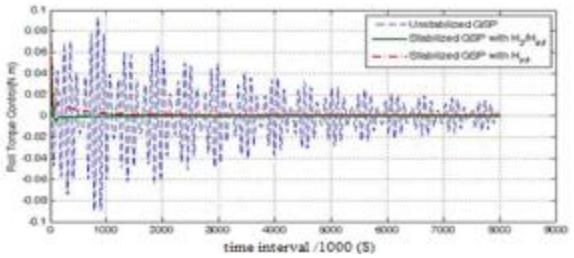

(a). Roll

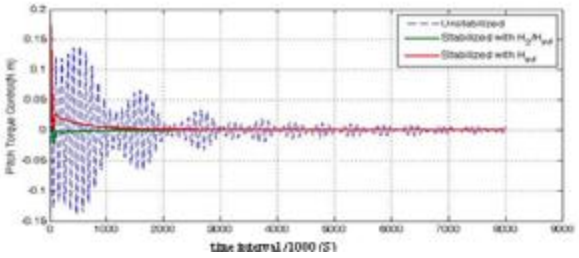

(b). Pitch

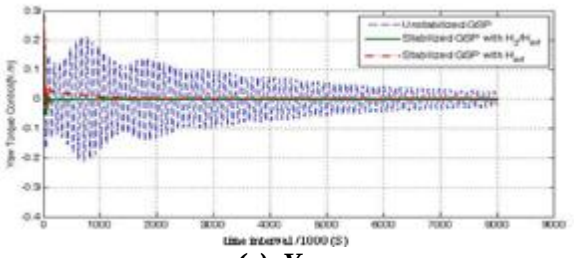

(c). Yaw

Figure 7. Channels Control Command Comparison With and Without GSP Stabilizing

In the second step, the idea of system stabilizing with the use of an inner loop with application of error and its rate of changes for the proposed $\mathcal{H}_2/\mathcal{H}_\infty$ controller is implemented. In this section, as shown in 0, the inner loop stabilized system with minimum control effort with maximum disturbance rejection, and the outer loop achieves the tracking objective with the help of error changes. The simulations show that this idea is very appropriate for the system and platform in tracking process to have an accurate stable situation. The tracking and control effort comparison are shown in 0and 0.

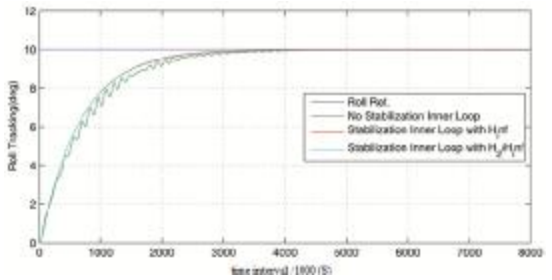

(a).Roll

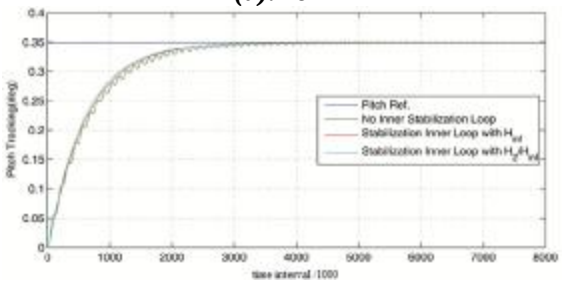

(b).Pitch

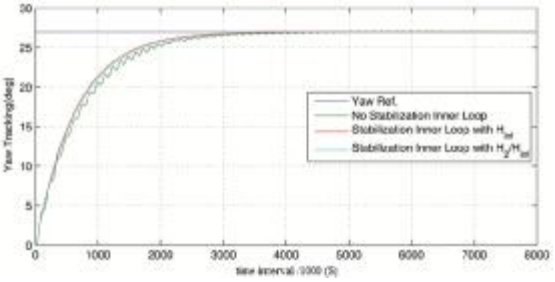

(c).Yaw

Figure 8. Implementation of integrated controller with platform stabilizing

Main characteristics of the proposed controller show its advantages. This makes it more preferable than the other controllers as to be optimal, and compensate disturbances and uncertainty of the system. So, to show these characteristics in controlled system with NLPID and proposed controller, a known disturbance has been exerted to system and with equal tracking trajectory, generated control moment to each channel compared. Finally, the results of comparison of controller simulations are as table 1.

Table 1.Simulation result comparison of controllers

Controller	Control effort RMS	Performance improvement with control effor increase
NLPID without stab.	19.67	-
$\boldsymbol{MPC/\mathcal{H}_\infty}$	13.08	33.5%
$\boldsymbol{ID\ MPC/\mathcal{H}_\infty}$	14.17	27.96%
$\boldsymbol{MPC/\mathcal{H}_\infty - \mathcal{H}_2}$	10.91	44.5%
$\boldsymbol{ID\ MPC/\mathcal{H}_\infty - \mathcal{H}_2}$	12.02	38.9%

Comparison results of simulation of this controller on plant with uncertainty are shown in following figures. This comparison shows the effect of integral/derivative in compensating disturbance and uncertainty.

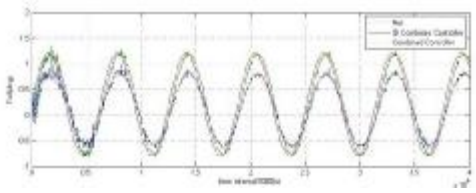

(a). roll

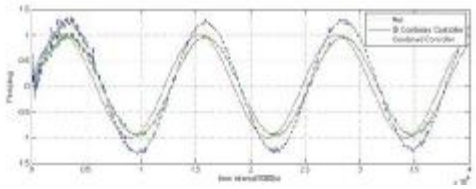

(b). pitch

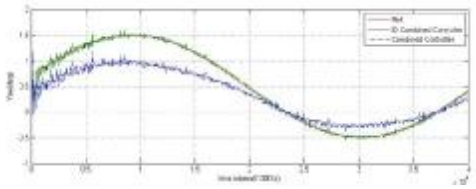

(c). yaw

Figure 9. Tracking with disturbance and uncertainty

Controller Implementation in KNTU Laboratory

A 3-axis GSP is set up in navigation laboratory of KNTU. To ensure the reliability and performance of proposed controller, it is implemented on this real time system. Because of delay dependent system, proposed MPC has a good performance on the system. To set up this system a fiber carbon structure and 3 servo motors is used. A schematic view of this structure is shown in figure 10.

Figure 10.3-axis camera stabilizer conceptual design

Specifications of these parts specified in table 2.

Table 2. Platform specifications

Body material	*Carbon fiber & plastic*
Mass	*250 gr.*
Pitch servo motor (Alware-Hitec)	
Speed	*60 deg. in 0.07 sec.* *857 deg/s in 4.8 V*
Torque	*0.373 N.m in 4.8 V* *0.471 N.m in 6 V*
Size	*29.4*15*35.6 mm*
Mass	25 gr.
Yaw & Roll servo motor (Alware-Hitec)	
Speed	60 deg in 0.16 sec. 375 deg/s in 4.8 V
Torque	0.981 N.m in 4.8 V 1.18 N.m in 6 V
Size	38*20*40 mm
Mass	50.3 gr.

An AHRS sensor to measure platform attitude changes is mounted on the platform. The AHRS sensor specification which is used in this platform specified in table 3.

Table 3. Space AHRS sensor

size	*23*23*2.2 mm*
Mass	*0.3 gr*
Power supply	*+3.3v ~ +6.0v*
Power consumption	*45mA @ 5v*
Connection port	*USB 2.0, SPI, Asynchronous Serial*
Output attitudes	*Quaternion, Euler angles,axis angle, rotation matrix, raw-corrected-normalized sensor data*
Serial bude rate	*1200-921600*
Max. shock	*5000 g*
Temperature range	*-40 to 85 Celsious*
Attitude measurement range	*360 deg about all axis*
Orientation accuracy	*±2º for dynamic conditions & all orientations*
Orientation resolution	*<0.08º*
Orientation repeatability	*0.085º for all orientations*
Accelerometer scale	*±2g / ±4g / ±8g selectable*
Accelerometer sensitivity	*0.00024g/digit for ±2g range 0.00048g/digit for ±4g range 0.00096g/digit for ±8g range*
Gyro noise density	*0.03º/sec/Ö Hz*
Gyro bias stability @ 25°C	*11º/hr average for all axes*
Gyro sensitivity	*0.00875º/sec/digit for ±250º/sec 0.01750º/sec/digit for ±500º/sec 0.070º/sec/digit for ±2000º/sec*
Compass sensitivity	*5 mGa/digit*

Parts of this MEMS sensor with serial and USB connection port introduced in figure 11 and figure 12.

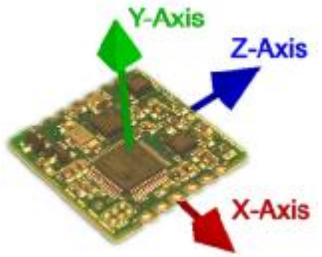

Figure 11.MEMS 3-Space sensor

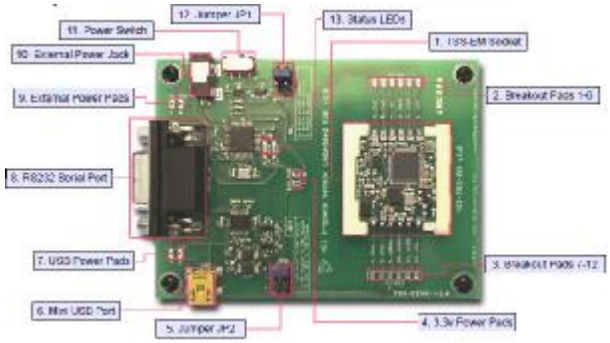

Figure 12.-space Connection module of MEMS to PC with RS232 and USB

Finally servo control board and its specification introduced in table 4 and figure 13. This board could control 32 servo motor instantaneously. Here 3 channels have been used that with a USB port has been connected to MATLAB.

table 1. Servo motors control driver spec.

Servo driver spec. No.	*DF-USBSSC-32*
Microcontroller	*Atmel ATMEGA168-20PU*
Servo control	*Up to 32 servos plug in directly*
Input voltage	*6V*
Servo type supported	*Futaba or Hitec*
PC interface	*USB*

Figure 13. Servo motors control driver card with USB port

This set up has been implemented in MATLAB environment for AHRS data acquisition and control servo motors. MATLAB code to read sensor data is as:

```
sensor = serial('COM7','BaudRate',115200);

fopen(sensor);
fprintf(sensor,':1\');

result = fscanf(sensor);
result = textscan(result,'%f32,%f32,%f32')';

result=cell2mat(result)*180/pi;

roll=result(1);pitch=result(3);yaw=result(2);

fprintf(sensor,':33\');

result = fscanf(sensor);

result = textscan(result,'%f32,%f32,%f32');

result=cell2mat(result);

roll_d=result(1);pitch_d=result(3);yaw_d=result(2);
```

And mfile code to send feedback to servo motors is:

```
temporary1 =
sprintf('#0P%dT500#1P%dT500#2P%dT500'...
   ,position1,position2,position3);

fprintf(S,temporary1)

fclose(s)
```

Finally, the structure that is mounted on a camera stand is shown in figure 14. In the following figures, red, green and purple boxes show the servo motors, AHRS and camera mounted on the platform.

(a)

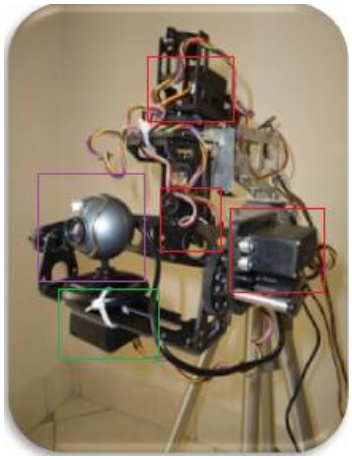

(b)

Figure 14. KNTU lab. 3-axis GSP set up

The results of implementation of the proposed controller in the real time system generated as follows:

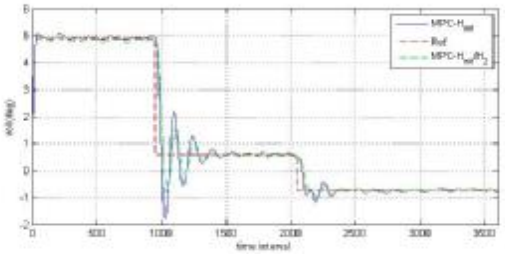

(a).Roll

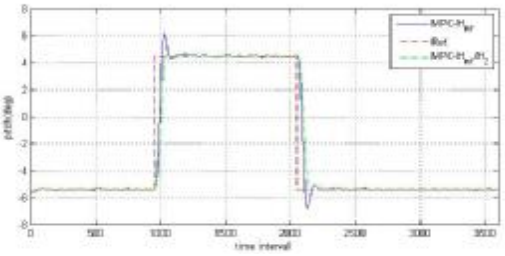

(b).Pitch

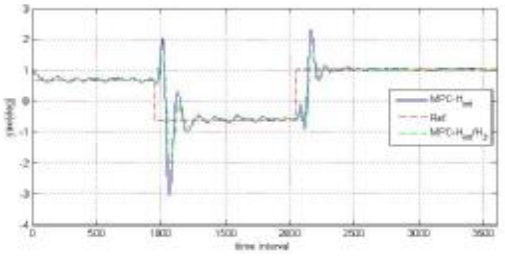

(c).Yaw

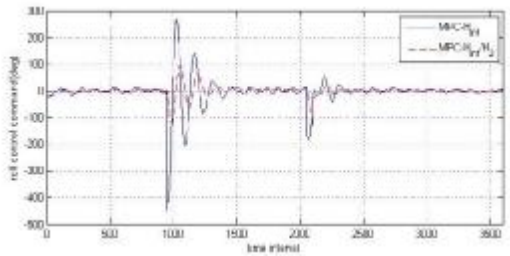

Figure 15. (d). roll control force

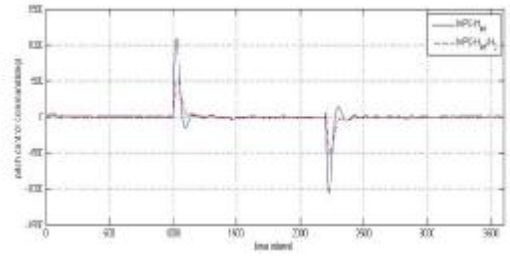

Figure 1 16.(e).pitch control force

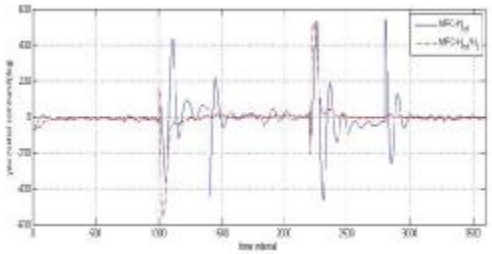

Figure 17.(f). yaw control force

Figure 18. Implementation of integrated controller with platform stabilizing

To show robustness of the designed system, attitude change of platform at the same time for all of channels considered. Uncertainties and disturbances affected on each channel. This process shows the robustness of the system against unknown sudden changes.

These results in the laboratory shows the performance improvement of 3-axis GSP as the same trajectory is tracked in both configuration, many energy is saved by applying $\mathcal{H}_2/\mathcal{H}_\infty$ controller.

Conclusion

The GSP has an oscillated line of sight, which complicates its control. The results show the effectiveness of the $\mathcal{H}_2/\mathcal{H}_\infty$ optimal controller in the presence of disturbances and uncertainty in theory and real time system to have disturbance rejection. Minimum power consumption of the proposed controller compared with the $\mathcal{H}_\infty$ sub-optimal and NLPID controller.

The results show that the proposed controller is robust against disturbance and uncertainties. This characteristic is very important for this system to be controlled by smaller servo motors.

NOMENCLATURE			
D	Damping coefficient about output axis	T_{di}	External disturbance torque of related axis
F_i	Servo-amplifier transfer function	T_{ni}	Net input torque of related axis
$\dot{H}$	Moment of applied torque	T_{si}	Servo torque of related axis
H_x	Gyro angular momentum	U_C	Control input
H_y	Angular momentum of y axis gyro	$\bar{U}_0$	Reference input
H_z	Angular momentum of z axis gyro	U_f	Desired applied input
$i: x, y, z$	Related axis representation	U_{Pi}	Net applied output torque
I_i	Total moment of inertia about output axis	Y_P	Plant output
J_i	Total moment of inertia about input axis	f	Input angle of gyro
K	Spring constant about output axis	s_i	Absolute angular motion about output axis
$k(x,t)$	external structured disturbance nonlinear dynamic	ω	Input axis rate of rotation
M	Output gyro moment	q	Output angle of gyro
$n(x,t)$	unstructured external disturbance nonlinear dynamic		

References

[1] *Gustavo J. Pereira and Humberto X. de Ara´ujo, "Robust Output Feedback Controller Design via Genetic Algorithms and LMIs: The Mixed H_2/H_∞ Problem",* ***Proceeding of the 2004 American Control Conference Boston, Massachusetts****, June 30 - July 2, (2004)*

[2] *William C. Reigelsperger Jr., "Direct Reduced Order Mixed H_2/H_∞ Control For The Short Take-Off and Landing Maneuver Technology Demonstrator (Stol/Mtd)" ,* ***Master Of Science In Aeronautical Engineering Theses, Air Force Institute Of Technology****, (1994)*

[3] *Carsten Scherer, "Mixed H_2/H_∞ Control", Mechanical Engineering Systems and Control Group Delft University of Technology*

[4] *Andrey Popov, "Less Conservative Mixed H_2/H_∞ Controller Design Using Multi-Objective Optimization", **Technical University of Hamburg**, (2005)*

[5] *Ali Saberi, Ben M. Chen, Peddapullaiah Sannuti, "Simultaneous H_2/H_∞ Optimal Control: The State Feedback Case", **Automatica**, Vol. 29, (1993), No. 6, 1611-1614*

[6] *R. Scott Erwin, Dennis S. Bernstein, "Fixed-Structure Discrete-Time H_2/H_∞ Controller Synthesis Using The Delta Operator", **Int. J. Control**, Vol. 75,(2002), No. 8, 559-571*

[7] *Pierre Apkarian, Dominikus Noll and Aude Rondepierre, "Mixed H_2/H_∞ control via nonsmooth optimization",* **Conference on Decision and Control-CDC**, (2009), 6460-6465

[8] *V. A. Mut, J. F. Postigo, R. O. Carelli, B. Kuchen ,"*Robust Hybrid Motion Force Control Algorithm for Robot Manipulators", **IJE,** *Vol. 13(4), 55-64, (2000)*

[9] *C. Poussot-Vassal, O. Sename, L. Dugard, P. Gáspár, Z. Szabó, J. Bokor, "Multi-objective qLPV H_2/H_∞ control of a half vehicle", **10th Mini Conference on vehicle system dynamics, identification and anomalies, VSDIA, Budapest :Hungary**, (2006)*

[10] *Riccardo Muradore, Giorgio Picci, "Mixed H_2/H_∞ Control: the Discrete-Time Case", **Proceedings of the 42nd IEEE Conference on Decision and Control Maui, Hawaii USA**, December (2003)*

[11] *Yang Wang and Stephen Boyd, "Fast Model Predictive Control Using Online Optimization", **IEEE Transactions on Control Systems Technology**, Vol. 18, (2010), NO. 2*

[12] *Guilherme V. Raffo, Manuel G. Ortega, Francisco R. Rubio, "An integral predictive/nonlinear H_∞ control structure for a quadrotor helicopter", **Automatica**, No.46,(2010), 29-39*

[13] *Camacho, E., & Bordons, C., "Model predictive control", **New York: Springer-Verlag**, (1998)*

[14] *Leonardo L. Giovanini, "Predictive feedback control", **ISA Transactions**, Vol.42, (2003), 207–226*

[15] *T. MITSUTOMI, J. M. Slater and D. B. Duncan, "Characteristics and Stabilization of an Inertial Platform", **Inertial Navigation, Aeronautical Eng. Rev.**, Vol. 15, (1956), 49-53*

[16] *Van der Schaft, A., "L_2 gain and passivity techniques in nonlinear control", **NewYork: Springer-Verlag**, (2000)*

[17] *Wen-Ben Wu, Pang-Chia Chen, Min-Hsiung Hung, Koan-Yuh Chang, Wen-Jer Chang, "LMI Robustly Decentralized H∞ Output Feedback Controller Design for Stochastic Large-Scale Uncertain Systems With Time-Delays", **Journal of Marine Science and Technology**, Vol. 17(1),(2009), 42-49*

[18] *J.C. Geromel, P.L.D. Peres and S.R. Souza,"Convex A006Ealysis of Output Feedback Control Problems: Robust Stability and Performance", **IEEE Transactions on Automatic Control**, Vol. 41(7), (1996), 997-1003.*

[19] *Carsten Scherer, Pascal Gahinet, Mahmoud Chilali, "Multiobjective Output-Feedback", Control via LMI Optimization, **IEEE Transactions on Automatic Control**, Vol. 42(7), (1997)*

[20] *A.M. Abdel Ghany, Ahmed Ghazi Alghmdi, "Mixed H_2/H_∞ with Pole-Placement Design of Robust LMI-Based Output Feedback Controller for A.C Turbo-Generator Power System Connected to Infinite Bus", **Proceedings of the 5th Saudi Technical Conference & Exhibition, STCEX'2009, Riyadh, Saudi Arabia**, January. 11-13, (2009).*

[21] *Pascal Gahinet, Arkadi Nemirovski, Alan J. Laub, Mahmoud Chilali," LMI MATLAB Control Toolbox", **The Math Works, Inc**, (1995)*

[22] مهدی رضایی دارستانی، امیرعلی نیکخواه، کنترل صفحه پایدار ژیروسکوپی سه محوره دوربین بکمک کنترلر PID غیرخطی، دهمین انجمن هوافضای ایران، اسفند 1389

[23] *M. Rezaei Darestani, A. A. Nikkhah, A Khaki Sedigh, H_∞/Predictive output control of a three-axis gyrostabilized platform, **Proceedings of the Institution of Mechanical Engineers, Part G: Journal of Aerospace Engineering**, 2013*

[24] *M. Rezaei Darestani, A. A. Nikkhah a, A. Khaki Sedigh, predictive controlled GSP performance improvement with an integrated H_2/H_∞, **IJE TRANSACTIONS B: Applications Vol. 26, No. 11**, 2013.*